



Tectonics, tectonophysics

## Structural evolution of metamorphic rocks in the Talas Alatau, Tien Shan, Central Asia: Implication for early stages of the Talas–Ferghana Fault

*Évolution structurale des roches métamorphiques du Talas Alatau, Tien Shan, Asie centrale : implication pour les stades précoces de la Faille du Talas–Ferghana*

Viacheslav N. Voytenko<sup>\*</sup>, Andrey K. Khudoley

St. Petersburg State University, Geological Department, University Nab. 7/9, St. Petersburg, 199034, Russia

## ARTICLE INFO

## Article history:

Received 16 February 2011

Accepted after revision 10 November 2011

Available online 29 March 2012

Written on invitation of the  
Editorial Board

## Keywords:

Early Paleozoic

Strain analysis

Buckling

Flattening

Deformation events

Talas–Ferghana Fault

Central Asia

## Mots clés :

Paléozoïque inférieur

Analyse de contrainte

Gauchissement

Aplanissement

Déformation

Faille de Talas–Ferghana

Asie centrale

## ABSTRACT

The Talas Alatau Ridge consists of three tectonic units separated by thrusts. The central (Talas parautochthon) and northeastern (Kumyshtag sheet) parts consist mainly of unmetamorphosed terrigenous and carbonate deposits. The southwestern part of the Talas Alatau (Usunakhmat sheet) consists of greenschists and is bounded by the Central Talas Thrust (CTT) and Talas–Ferghana Fault (TFF). The latter is a major strike-slip fault with post-Permian dextral displacement estimated at as much as 200 km. A structural study shows that elongation axes of strain ellipsoids, stretching lineation and map-scale fold axes, as well as the trend of major faults including the CTT and the TFF, are parallel to each other. The natural deviatoric strain value gradually increases from the CTT to the TFF. The shape of the strain ellipsoid gradually varies within the Usunakhmat sheet from oblate at the frontal thrust to prolate in internal parts of the unit. The magnitude of shortening increases towards the CTT, whereas natural deviatoric strain decreases towards the CTT implying structural thickening of internal parts of the Usunakhmat sheet. Strong parallelism of the TFF, CTF and other map- and outcrop-scale structures and their close connection with strain patterns show that they were formed during the same tectonic event. They were likely formed during Middle to Late Ordovician collision and built up Kyrgyzian microcontinent as a thrust fold belt whereas reactivation of the TFF as a strike-slip fault occurred later, in Late Paleozoic.

© 2012 Académie des sciences. Published by Elsevier Masson SAS. All rights reserved.

## R É S U M É

La Chaîne de Talas Alatau consiste en trois unités tectoniques séparées par des charriages. Les parties centrale (parautochtone de Talas) et nord-orientale (unité de Kumyshtag) sont constituées essentiellement de dépôts carbonatés et terrigènes non métamorphosés. La partie sud-occidentale du Talas Alatau (unité d'Usunakhmat) consiste en schistes verts et est limitée par le charriage central de Talas (CTT) et par la Faille de Talas–Ferghana (TFF). Cette dernière est un décrochement majeur, avec déplacement dextre post-Permien, estimé à environ 200 km. L'étude structurale montre que les axes d'élongation des ellipsoïdes de contrainte et les axes de plis à l'échelle de la carte, ainsi que la déformation des failles majeures incluant CTT et TFF sont parallèles les uns par rapport aux autres. La valeur naturelle de la contrainte de déviatorique augmente graduellement de CTT à TFF. La

<sup>\*</sup> Corresponding author.

E-mail address: [vaclav.vojtenko@gmail.com](mailto:vaclav.vojtenko@gmail.com) (V.N. Voytenko).

forme de l'ellipsoïde de contrainte varie aussi graduellement, au sein de l'unité d'Usunakhmat, d'oblate au front du charriage à prolatae dans les parties internes de l'unité. L'amplitude du raccourcissement augmente vers CTT, tandis que la contrainte déviatorique naturelle décroît vers CTT impliquant un épaississement structural des parties internes de l'unité d'Usunakhmat. Un parallélisme intense de TFF, CTF et d'autres structures à l'échelle de la carte ou de l'affleurement et leur connexion étroite avec les configurations de contrainte montrent que TFF et CTF se sont formés pendant le même événement tectonique : leur genèse a vraisemblablement pris place lors de la collision à l'Ordovicien moyen-supérieur et donné naissance au microcontinent Kyrgyzian en tant que ceinture plissée de charriage, alors que la réactivation de TFF en tant que faille de décrochement s'est produite plus tard, au Paléozoïque supérieur.

© 2012 Académie des sciences. Publié par Elsevier Masson SAS. Tous droits réservés.

## 1. Introduction

The Talas-Ferghana Fault (TFF) is located in the western part of the Tien Shan mountains (Central Asia) and is one of the world's largest strike-slip faults located on the continental crust with dextral displacement up to 200 km (Burtman, 1975, 1980, 2006; Burtman et al., 1996). Its northwest continuation is the Main Karatau Fault (MKF), whereas southeastward it cuts Caledonian and Hercynian structures of the Middle and southern Tien Shan (Fig. 1a). The age of the TFF and the MKF is not clear, but, according to data on the displacement of Paleozoic and younger rocks, it is commonly assumed that the dextral displacement started in the Permian. However, Khudoley and Semiletkin (1992a) interpreted the TFF, Central Talas Thrust (CTT) and northeast-vergent thrusts as a single imbricate thrust fan, formed in the Early Paleozoic with the Late Paleozoic reactivation of the TFF as a strike-slip fault.

Starting from Karatau in the north, up to the Naryn part of the Middle Tien Shan in the south, metamorphic rocks of greenschist to amphibolite grade are distributed mainly in the northeastern side of the MKF and TFF faults. The age of metamorphic rocks was traditionally assumed as Neoproterozoic (Abad et al., 2003; Bakirov and Dobretzov, 1972; Becker et al., 1988; Chakabaev, 1979; Kiselev and Korolev, 1981; Sagyndykov, 1964). However, sedimentary units correlation based on the detailed structural and sedimentological studies as well as rare findings of fauna fossils give evidence for a Paleozoic age of the metamorphic rocks (Khudoley and Semiletkin, 1992a; Kiselev and Maksumova, 2001; Maksumova et al., 2001).

Although structural studies in the study area and adjacent regions were done by many researchers (Abad et al., 2003; Alexeiev et al., 2009; Becker, 1987; Burtman, 1975; Burtman et al., 1996; Frolova, 1982; Goncharov, 1998; Khudoley and Semiletkin, 1992a; Yakovlev, 1976), strain patterns were discussed only in a few papers (Khudoley, 1993; Pastor-Galán et al., 2009; Voytenko et al., 2006). The main goal of this article is to discuss structures and strain patterns of the metamorphic rocks located in the central part of Talas Alatau Ridge with emphasis on the strain analysis and relationship between the TFF and other structures of the metamorphic rocks that will help to understand the early evolution of the TFF.

## 2. Geological background

### 2.1. Regional setting

The Talas Alatau Ridge is located in the northwestern part of the Republic of Kyrgyzstan. The main tectonic and stratigraphic features of the region are shown in Figs. 1 and 2.

Most of the Talas Alatau Ridge belongs to the southeastern part of the Caledonian Talas-Karatau zone of the northern Tien Shan (Fig. 1b). Its southwest boundary is the TFF, which separates it from the Hercynian Middle Tien Shan, whereas the Ichkeletau-Susamyr Fault separates it from the northern Tien Shan Caledonides (Kokchetav-northern Tien Shan microcontinent) in the northeast (Fig. 1c) (Maksumova et al., 2001).

The Caledonian part of the Talas Alatau Ridge discussed in this article consists of three tectonic units (Khudoley, 1993; Khudoley and Semiletkin, 1992a). The lowermost unit is exposed in its central part and is interpreted as parautochthon or autochthon (Talas parautochthon, Figs. 1c and d). It consists of a coarsening-upward terrigenous succession deposited in submarine fan to shelf environments with some carbonate units in its central part (Fig. 2). The total thickness of the succession is estimated as 5 to 6 km. The age of the succession was traditionally accepted as Neoproterozoic (Abad et al., 2003; Becker et al., 1988; Kiselev and Korolev, 1981). However, findings of rare fauna fossils show that at least the upper part of the succession is as young as Cambrian to Middle Ordovician in age (Fig. 2) (Khudoley and Semiletkin, 1992a; Kiselev and Maksumova, 2001; Maksumova et al., 2001; Semiletkin, 2007 and references therein). It resulted in a significant revision of ideas on the structure and evolution of the Talas parautochthon. Metamorphic alteration of rocks is low and gradually increases southwestward (Abad et al., 2003; Frolova, 1982). Thus, in the northeastern exposures of terrigenous rocks, cleavage was only documented in slate, whereas in the southwestern exposures cleavage is widespread in both slate and sandstones. More intense metamorphism up to biotite sub-grade was only documented around the Babakhan plagiogranite intrusion.

The Kumyshtag sheet consists of Latest Neoproterozoic non-marine and shallow marine siliciclastics with subordinate acid tuffs and Cambrian to Middle Ordovician

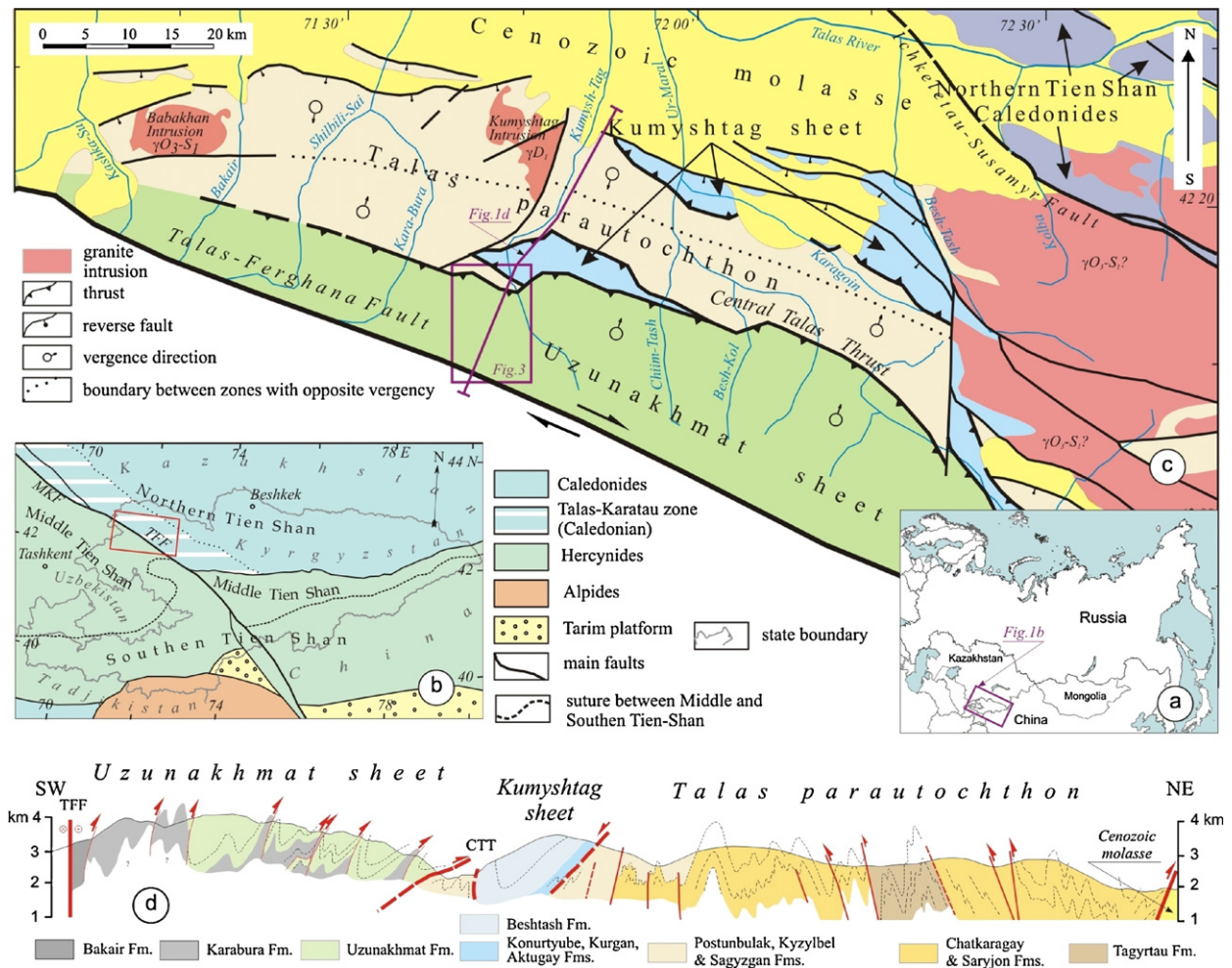


Fig. 1. Location map (a), regional setting (b) and tectonic map (c) of the Talas Alatau Ridge (after Khudoley, 1993; Khudoley and Semiletkin, 1992a; Tursungaziev and Petrov, 2008 and references therein). Rectangular indicates the study area. Regional cross-section (d) across the Caledonian part of the Talas Alatau (after Abad et al. 2003; Goncharov, 1998; Khudoley, 1993; Khudoley and Semiletkin, 1992a, modified). See Fig. 2 for stratigraphic correlations.

Fig. 1. Carte de localisation (a), cadre régional (b), carte tectonique (c) de la chaîne de Talas Alatau (selon Khudoley, 1993 ; Khudoley et Semiletkin, 1992a ; Tursungaziev et Petrov, 2008 et références incluses). L'encart indique la région étudiée. Coupe régionale (d) au travers de la partie calédonienne de la chaîne de Talas Alatau (selon Abad et al. 2003 ; Goncharov, 1998 ; Khudoley, 1993 ; Khudoley et Semiletkin, 1992a, modifié). Voir Fig. 2 pour les corrélations stratigraphiques.

shallow marine carbonates (Fig. 2). It is thrust south-westward over the Talas parautochthon. It is also widespread in the eastern part of the Talas Alatau ridge, where it constitutes a large tectonic klippe in its central part (Figs. 1c and d).

The main study area of this article is located within the Usunakhmat sheet, which is thrust northeastward over both Talas parautochthon and Kumyshtag sheet (Figs. 1c and d). It consists of terrigenous and carbonate rocks. These rocks correlate with those from the Talas parautochthon (Fig. 2), but are metamorphosed in the greenschist and, close to the TFF, in the amphibolite facies. Primary sedimentary structures are locally recognized, but often cannot be distinguished (Maksumova et al., 2001; Maluzhinetz, 1987). The metamorphic event is not yet dated, but correlation of metamorphic units with Neoproterozoic–Early Paleozoic succession of the Talas parautochthon

(Fig. 2) shows that metamorphic event was post-Middle Ordovician. Structural-metamorphic zonation is sub-parallel to the TFF (Frolova, 1982) and metamorphic alteration increases southwest towards the TFF (Abad et al., 2003; Frolova, 1982). Towards the southwest, the TFF bounds the Usunakhmat sheet, whereas its northeastern boundary is the CTT separating the Usunakhmat sheet from the Talas parautochthon and Kumyshtag sheet. Northwestward the CTT splits into several faults, whereas boundary between the Usunakhmat sheet and the Talas parautochthon evolves into a transitional zone (Goncharov, 1998; Khudoley and Semiletkin, 1992a; Yakovlev, 1976).

## 2.2. Structural styles of the Talas Alatau

The structural style of the Usunakhmat sheet is shown in cross-sections and maps (Figs. 1d, 3 and 4). It is

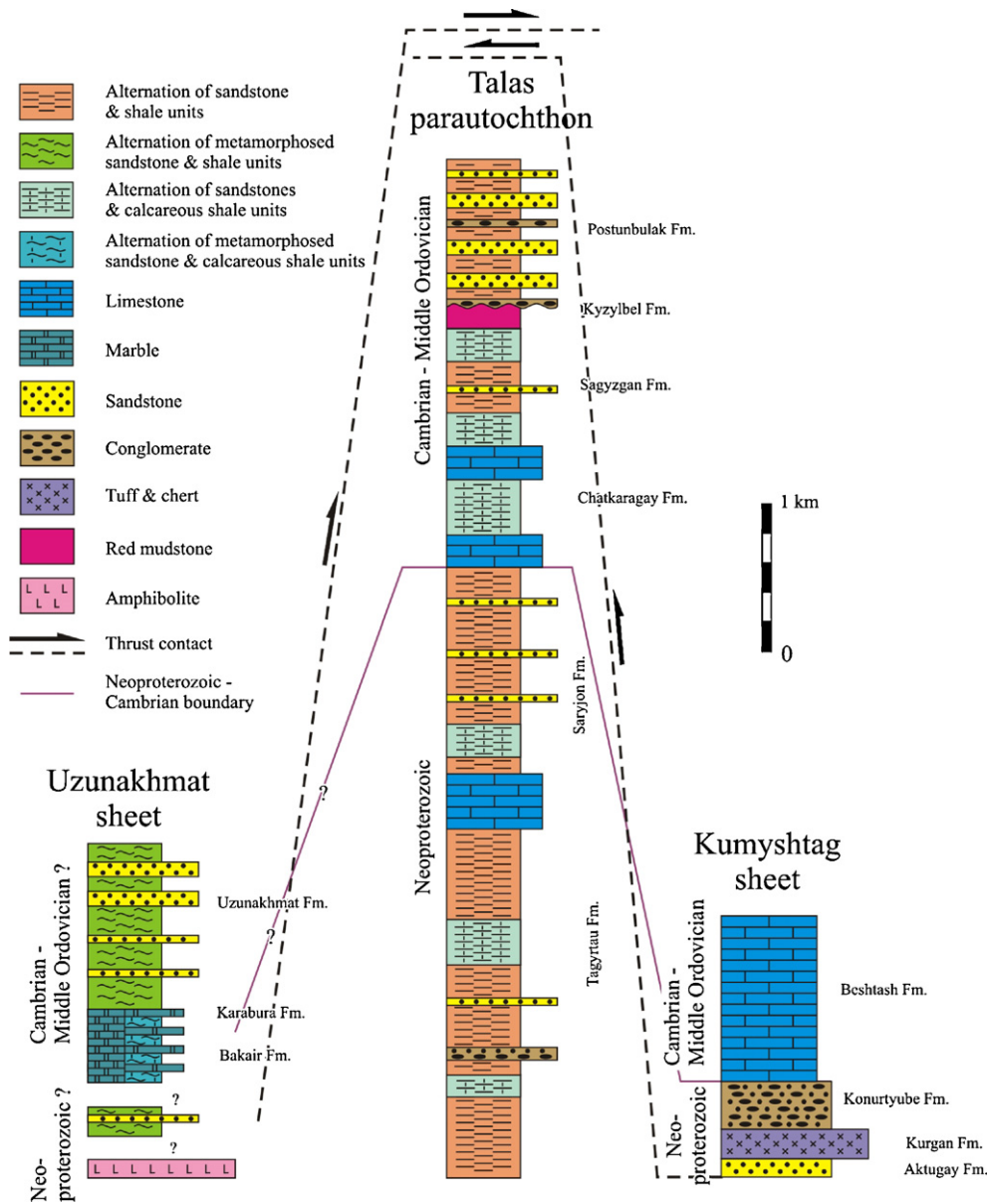


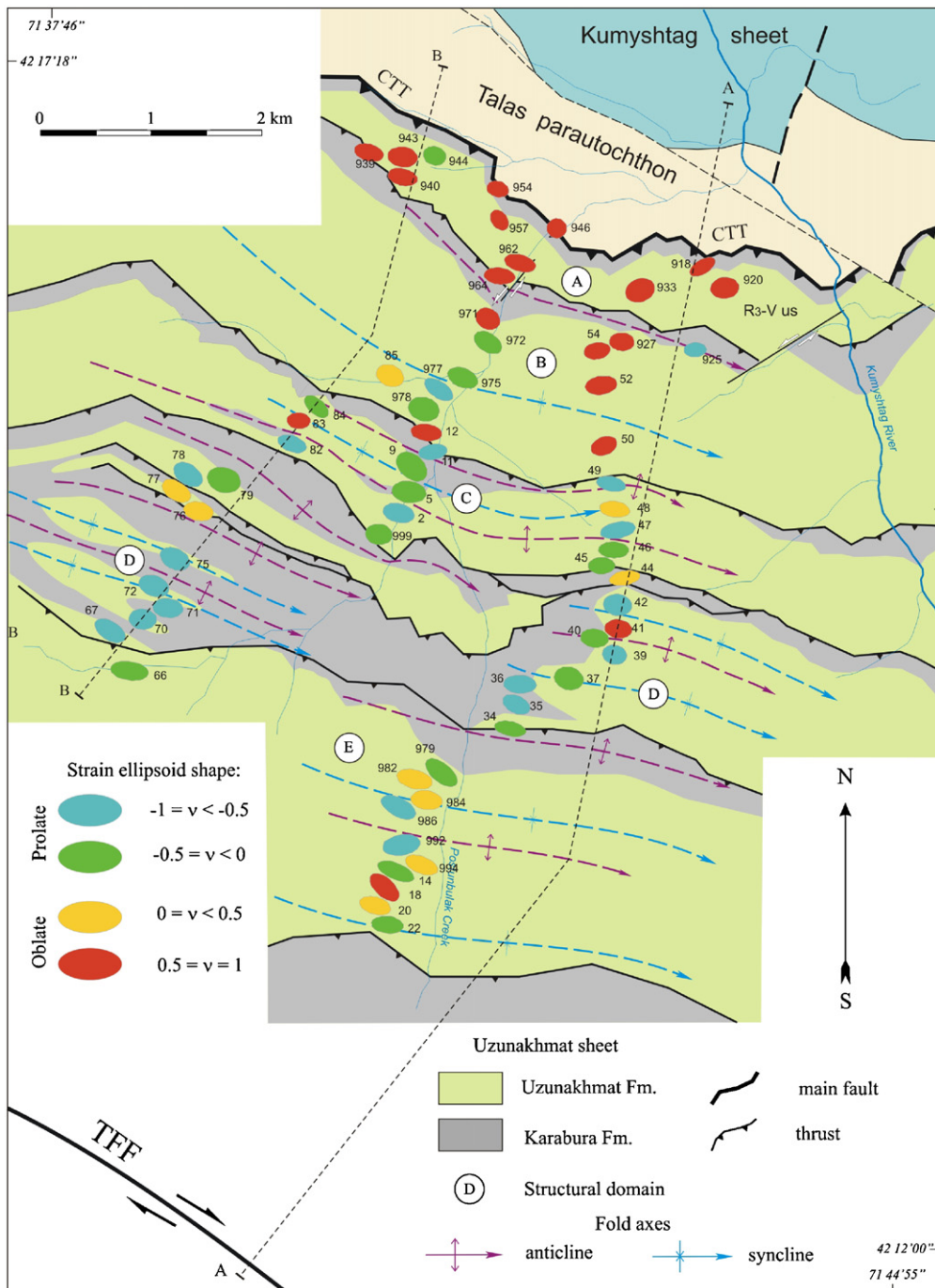
Fig. 2. Stratigraphy of the Talas Alatau ridge (Becker et al., 1988; Khudoley, 1993; Khudoley and Semiletkin, 1992b; Kiselev et al., 1986 and references therein), modified. Thickness of sedimentary units (see bar scale) not corrected for strain.

Fig. 2. Stratigraphie de la chaîne de Talas Alatau (Becker et al., 1988; Khudoley, 1993; Khudoley et Semiletkin, 1992b; Kiselev et al., 1986 et références incluses), modifié. Épaisseur des unités sédimentaires (voir barre d'échelle), non corrigée en fonction de la déformation.

controlled by the southwest-dipping imbricate thrusts and map-scale cylindrical folds which are overturned to the northeast (Abad et al., 2003; Becker, 1987; Khudoley, 1993; Khudoley and Semiletkin, 1992a). Dips of the folds axial planes and imbricate thrusts gradually increase from 40° to 45° near the CTT to subvertical near the TFF.

The shape and size of folds depend on the lithology of the beds. Thick sandstone and conglomerate units form folds up to 2 to 3 km in width, whereas units with thin interbedding of slate and sandstone or carbonate contain folds with predominant width varying from 10 cm to a few meters. However, folds axes of the map- and outcrop-scale

folds are almost parallel and gradually plunge to the southeast. The average dip of the fold axes is 5° to 7°, but the dip of some outcrop-scale fold axes is as high as 35°. Cleavage is widespread and typically parallel to the axial planes of the map-scale folds and imbricate thrust planes. However, in the eastern part of the Uzunakhmat sheet thrusts locally cut cleavage and fold axial planes, pointing to a continuation of thrust-related displacements after the end of folding (Becker, 1987). Cleavage-bedding intersection and stretching lineation, expressed by the preferred orientation of detrital grains in sandstone and conglomerates, are widespread and parallel to fold axes.



**Fig. 3.** Geological map (see Fig. 1c for location), shape and orientation of strain ellipsoids in the Uzunakhmat sheet. Ellipses on the map are horizontal section of strain ellipsoids. Color of the ellipses shows variations in Lode's parameter value  $v = \frac{(\epsilon_Y - \epsilon_Z) - (\epsilon_X - \epsilon_Y)}{(\epsilon_Y - \epsilon_Z) + (\epsilon_X - \epsilon_Y)}$ , where  $\epsilon_X \geq \epsilon_Y \geq \epsilon_Z$  – natural principal strains. Field numbers of samples are shown and correspond to numbers in the Table (Supplementary material).

**Fig. 3.** Carte géologique (voir Fig. 1c pour la localisation), forme et orientation des ellipsoïdes de contrainte dans l'unité d'Uzunakhmat. Les ellipses sur la carte représentent la section horizontale des ellipsoïdes de contrainte. La couleur des ellipses montre la variation de la valeur du paramètre de Lode  $v = \frac{(\epsilon_Y - \epsilon_Z) - (\epsilon_X - \epsilon_Y)}{(\epsilon_Y - \epsilon_Z) + (\epsilon_X - \epsilon_Y)}$ , où  $\epsilon_X \geq \epsilon_Y \geq \epsilon_Z$  – principales contraintes naturelles. Les numéros d'échantillons représentés correspondent aux numéros du Tableau (Matériel supplémentaire).

Small-scale strike-slip faults, kink-zones and crenulation cleavage folds have a local distribution. They cut folds and cleavages and are associated with dextral displacement along the TFF (Khudoley, 1993).

The structural style of the Talas parautochthon is dominated by numerous outcrop-scale folds which make identification of map-scale structures complicated (Fig. 1d). In the northeastern part of the Talas parautochthon, folds are overturned to the southwest with an axial plane dip varying from 80° to 50° (Becker, 1987; Khudoley and Semiletkin, 1992a). In the southwestern part of the Talas parautochthon, the southwest-verging folds are overprinted by folds overturned to the northeast.

The structural style of the Kumyshtag sheet is controlled by a wide distribution of a massive limestone unit of Cambrian to Middle Ordovician age (Figs. 1d and 2). Open folds and bedding-parallel detachments, located in the shale units, are most widespread. However, the mean orientations of the fold axes and axial planes are close to those in adjoining parts of the Talas parautochthon (Khudoley and Semiletkin, 1992a).

### 2.3. Deformation events of the Talas Alatau

Structural evolution of the Talas Alatau contains at least five stages of deformation (Khudoley, 1993; Khudoley and Semiletkin, 1992a). The first deformation stage is recognized in the northeastern and central parts of the region and is related to the southwestward displacement of the Kumyshtag sheet. The second stage had the same sense of shearing, but a local distribution, and resulted in the formation of southwest-vergent folds in the northeastern part of the Talas parautochthon.

Folds and thrusts of the Usunakhmat sheet were formed during the third deformation stage when the Usunakhmat sheet was thrust over both the Talas parautochthon and the Kumyshtag sheet, where already formed folds and faults were reworked by folds with northeast vergence. This third stage was accompanied by a greenschists metamorphic event. The fourth deformation stage corresponds to dextral displacements along the TFF and formation of locally distributed small-scale faults and minor structures which cut all map-scale folds and thrusts. The fifth stage of deformation is related to the Cenozoic Himalayan deformation. Uplift was coeval with the tectonic emplacement of thrusts of Paleozoic rocks over the Cenozoic molasse basin on the northeast margin of the Talas Alatau. The Himalayan deformation also resulted in rotation and re-orientation of some previous structures (Abad et al., 2003).

Folds and thrusts of the first two stages of deformation are cut by the Kumyshtag granite intrusion (Fig. 1c). U-Pb dating of zircons shows the occurrence of several clusters with the youngest aged at 400 Ma (Early Devonian), interpreted as the age of intrusion (Khudoley and Semiletkin, 1992a; Kiselev and Maksumova, 2001). In turn, the thrusts cut massive carbonates of the Beshtash Formation (Kumyshtag sheet), which are as young as Cambrian to Middle Ordovician in age (Fig. 2). These data constrain the age of deformation to between Middle Ordovician and Early Devonian.

The age of the third stage of deformation and the metamorphic event is poorly constrained, although similarity in trends of the third stage folds and thrusts with those from the first two stages implies that they are close in age. Deformations of the fourth stage are synchronous with dextral displacement along the TFF and are inferred to be Latest Permian in age or younger, whereas structures of the fifth stage correspond to the Cenozoic Himalayan deformation, resulting in regional-scale uplift and mountain building.

## 3. Strain analysis

### 3.1. Study area

The study area is located in the central part of the Usunakhmat sheet including the adjoining parts of the Talas parautochthon and Kumyshtag sheet (Fig. 1c and d). The compiled geological map and cross-sections show imbricate fan thrusts with cylindrical map-scale folds with southeast-plunging axes, which characterize the overall structural style of the Usunakhmat sheet (Figs. 3 and 4).

Five thrust-bounded structural domains are identified within the studied part of the Usunakhmat sheet (Figs. 3 and 4). The fold style depends on the domain width. In the two cross-sections shown in Fig. 4, folds have the same shape, whereas the domain width does not vary greatly (domains A, B, C, E). However, when width of domain decreases, folds become much tighter (domain D, Fig. 4). Folds located close to thrust planes are typically tighter than folds in the central parts of domains. Detailed mapping shows also that most folds and thrusts within the Usunakhmat sheet are parallel to the CTT and TFF which bound the sheet from northeast and southwest, respectively.

The stratigraphy of the study area is shown in Fig. 2, with two predominant units of sandstones and slates in the upper part of the succession (Usunakhmat Formation) and carbonates and slates in the lower part of the succession (Karabura Formation). Near the TFF a predominantly carbonate rock unit (Bakair Formation) is exposed, but it is not clear whether this unit or the highly strained Karabura Formation constitute the lowermost formation in the succession. In general, the lower part of the succession is exposed near the TFF, whereas most domains within the Usunakhmat sheet display the same stratigraphy.

### 3.2. Lithology and types of strain markers

Location of samples for strain analysis is shown in Figs. 3 and 4. The most widespread strain indicators are detrital grains in sandstones, and typical examples are shown in Fig. 5. Sampled sandstones are sub-lithic to lithic in composition and predominantly medium-grained. Sandstones are poorly sorted. Detrital grains are quartz (60 to 75%), plagioclase (andesine), potassium feldspar, muscovite, rutile, tourmaline, zircon and lithic clasts, i.e., quartzite, schists and volcanics. Grains have similar elongation forming mineral lineation identified in both thin sections and hand specimens. Quartz and some other grains have pressure shadows of quartz composition. Detrital grains are supported by matrix of chlorite, slate or calcareous slate

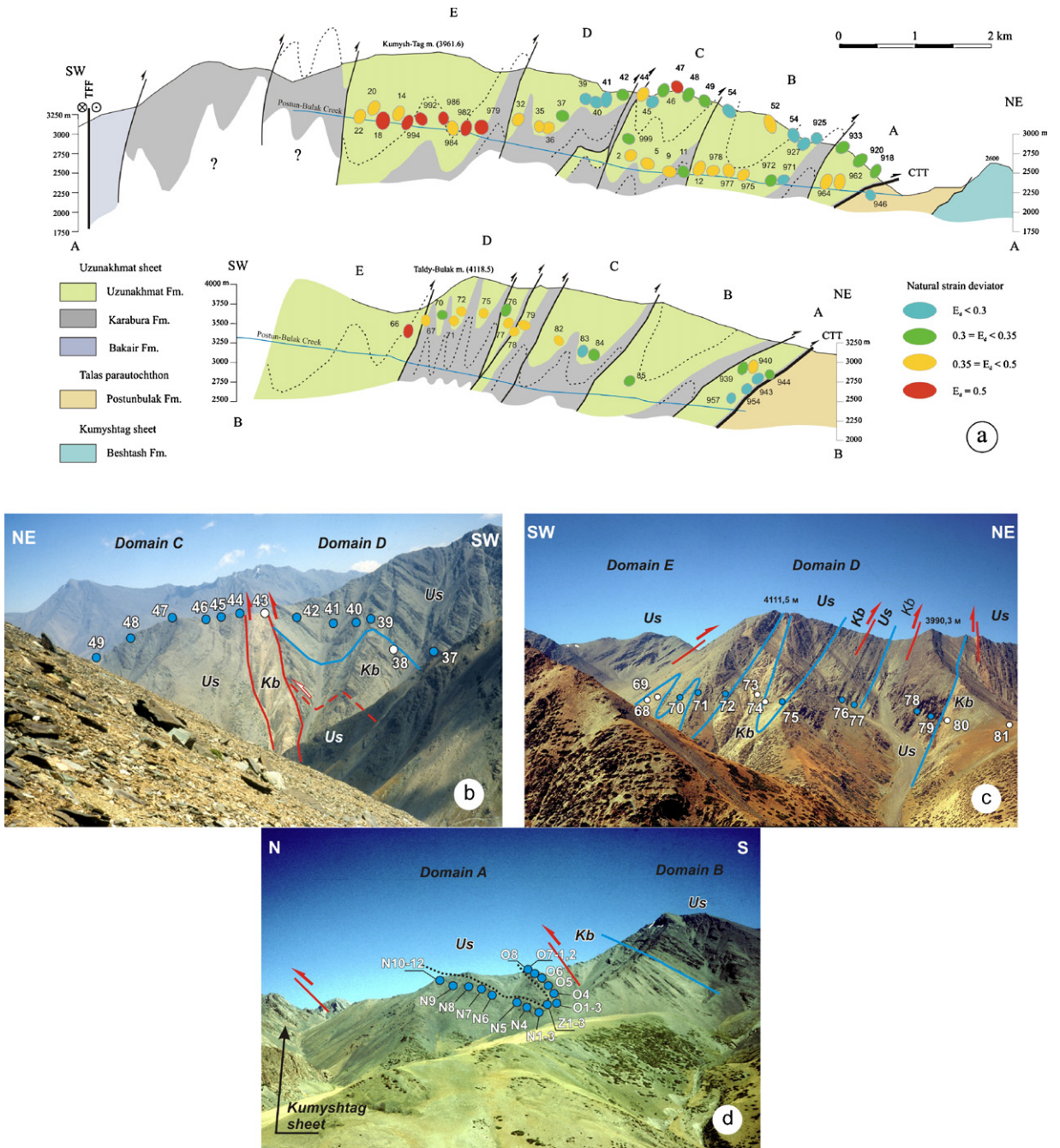


**Fig. 4.** Simplified cross-sections (Goncharov, 1998; Khudoley and Semiletkin, 1992a), modified, (see Fig. 3 for location) and natural strain deviator values in the Uzunakhmat sheet (a). Ellipses in cross-sections are vertical sections of strain ellipsoids. Colors of the ellipses show variation in natural deviatoric strain value  $E_d = \frac{1}{\sqrt{3}} [(e_X - e_Y)^2 + (e_Y - e_Z)^2 + (e_Z - e_X)^2]^{1/2}$ , where  $e_X \geq e_Y \geq e_Z$  - natural principal strains. Dotted lines are marker units. Field sample numbers are shown and correspond to numbers in the Table (Supplementary material). Structural style of the Uzunakhmat sheet (b, c and d). Uz; Uzunakhmat Fm.; Kb; Karabura Fm. The main thrusts and folds are outlined: b: east slope of the Postunbulak Creek valley; c: west slope of the Postunbulak Creek valley; d: east slope of Kumyshtag River valley. Blue lines are the contact between the Uzunakhmat Fm. and Karabura Fm., red lines correspond to thrusts. Blue spots show sample locations for strain analysis. Numbers on pictures are field station numbers corresponding with sample numbers in Table (Supplementary material). On all pictures the vertical relief is about 1500 m.

**Fig. 4.** Coupes simplifiées (Goncharov, 1998 ; Khudoley et Semiletkin, 1992a) et références incluses, modifié ; (voir Fig. 3 pour la localisation) et valeurs déviatoriques de contrainte naturelle dans le banc d'Uzunakhmat (a). Les ellipses sur les coupes représentent la section verticale des ellipsoïdes de contrainte. La couleur des ellipses montre la variation de la valeur de la contrainte déviatorique naturelle  $E_d = \frac{1}{\sqrt{3}} [(e_X - e_Y)^2 + (e_Y - e_Z)^2 + (e_Z - e_X)^2]^{1/2}$ , où  $e_X \geq e_Y \geq e_Z$  - principales contraintes naturelles. Les lignes en pointillés sont des éléments marqueurs. Les numéros d'échantillon correspondent aux numéros du Tableau (Matériel supplémentaire). Style structural de l'unité d'Uzunakhmat (b, c et d). Uz : Formation d'Uzunakhmat ; Kb : Formation de Karabura. Les principaux plis et

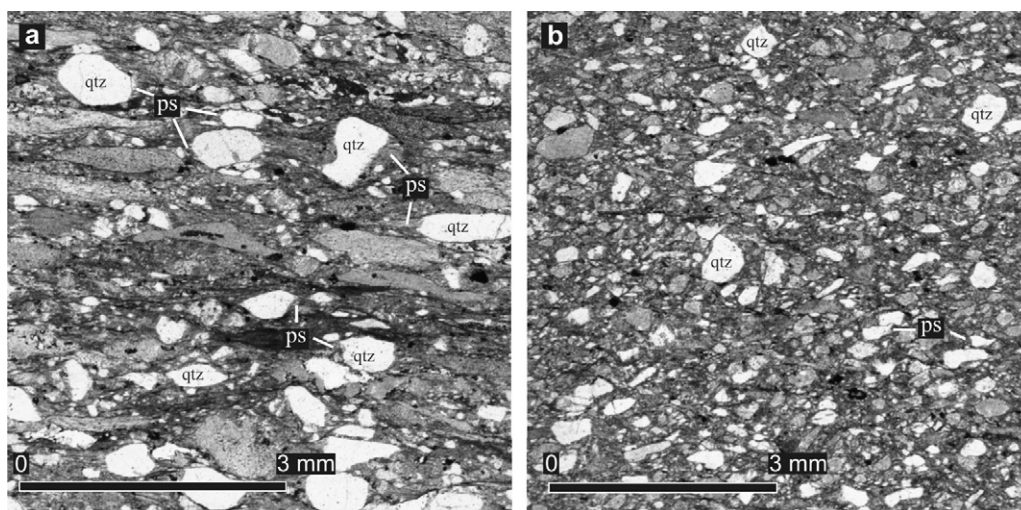


Fig. 5. Photomicrographs of meta-sandstones (XZ plane normal to cleavage and parallel to mineral lineation). Typical strain indicators are quartz grains (qtz) with pressure shadows (ps): a: sample # 46, strongly strained rock; b: sample # 918, weakly strained rock.

Fig. 5. Microphotographies de méta-grès (plan XZ perpendiculaire au clivage et parallèle à la linéation minérale). Les indicateurs de contrainte typiques sont les grains de quartz (qtz) avec ombrage de pression (ps) : a : échantillon # 46, roches très déformées ; b : échantillon # 918, roches faiblement déformées.

composition. Widespread cleavage shows pressure dissolution structures which affect detrital grains and the matrix.

### 3.3. Samples and methods of strain analyses

Samples for strain analysis were collected from central parts of sandstone beds similar in composition and more than 1 m thick. We collected 92 oriented samples in total, all from the Usunakhmat Formation (Figs. 3 and 4). Typically, two thin sections normal to the cleavage plane were produced from each sample to restore strain ellipsoid shape and orientation. One thin section was parallel and the other one was normal to the stretching lineation. The axial ratio in the third plane was calculated by equation  $R_{xy} = R_{xz}/R_{yz}$  (Ramsay and Huber, 1983). Three thin sections were produced from several samples to check the calculation accuracy. To avoid viscosity contrast problems only detrital quartz grains were studied.

At least 150 quartz grains were studied in each thin section, but typically the number of studied grains was 250 or higher. The actual shape of the quartz grains was approximated by ellipses using AutoCAD software which facilitated determination of the ellipse's center and end point coordinates used for the calculation of axial ratio and long axis orientation.  $R_f/\phi$ , MRL and ENFry methods of strain analyses with related software developed by Chew (2003), Mulchrone et al. (2003) and Erslev and Ge (1990) were used in the strain estimation.

Pressure shadows around detrital quartz grains were considered as a part of detrital grain for the strain estimation using  $R_f/\phi$  and MRL methods to decrease the

influence of volume loss, which is typical for rocks affected by pressure solution and cleavage formation (Dunne et al., 1990; Onasch, 1984). However, the ENFry method applied to the same grains with well-preserved initial boundaries showed very similar strain estimations assuming that volume did not significantly vary during the deformation event, and the formation of quartz fibers in pressure shadows was related to very local dissolution and precipitation without total volume variations. Preservation of the total volume, even at hand-specimen scale, is also shown by a very small variation of the chemical composition of the same bed affected by a different strain in a different part of the fold structure (Voitenko et al., 2006).

Estimations by  $R_f/\phi$  and MRL methods show very similar strain values that were insignificantly lower than those estimated by the ENFry method. However, for samples studied, strain estimations inferred by the MRL method show the least error. In the following text and Table (Supplementary material), we discuss results by the MRL method only.

### 3.4. Strain ellipsoid orientation and natural deviatoric strain variations

Results of the strain estimations are shown in Figs. 3 and 4, and in the Table (Supplementary material). Within the study area, the axis of shortening of the strain ellipsoid has a northeast trend, whereas the extension axis has a northwest trend. The latter is sub-parallel to the map-scale fold axes and the trend of thrusts and the TFF excluding

charriages sont surlignés ; b : versant oriental de la vallée de Postunbulak Creck ; c : versant occidental de la même vallée ; d : versant oriental de la vallée de la rivière Kumyshtag. La ligne bleue représente le contact entre les formations d'Usunakhmat et de Karabura, les lignes rouges, les charriages. Les points bleus montrent la localisation des échantillons utilisés pour l'analyse de contrainte. Les numéros sur les photos sont les numéros des stations de terrain correspondant aux numéros d'échantillons du Tableau (Matériel supplémentaire). Sur toutes les photos, le relief vertical est environ 1500 m.

only domain A adjoining to the CTT. The axis of shortening typically has a northeast trend near the CTT, whereas both extension and intermediate axes have variable orientations in the plane normal to the axis of shortening. Outside the CTT both extension and shortening axes are subhorizontal.

The shape of the strain ellipsoid is identified by the Lode parameter  $\nu$  (Ramsay and Huber, 1983) and is shown in Fig. 3. In the northern part, close to the CTT, oblate ellipsoid predominates, whereas towards the TFF the shape of strain ellipsoids gradually changes from an oblate to a prolate one. In all domains the most oblate ellipsoids were documented close to the basal thrust.

The axial ratio ( $R_s$ ) of strain ellipses in cross-sections compiled normal to the structural trend does not reflect the total strain. As in the Uzunakmat sheet, the extension axis is parallel to the folds axes (Khudoley, 1993). Therefore, we discuss variations of the natural deviatoric strain value ( $E_d$ ) that corresponds to the total strain variations.

The natural deviatoric strain  $E_d$  (Brandon, 1995) gradually decreases from the TFF to CTT (Fig. 4). However, near the CTT the deviatoric strain varies greatly from 0.10 to 0.44, whereas near the TFF it shows higher magnitude but less variation (0.35 to 0.52).

#### 4. Horizontal shortening estimation

Estimation of the shortening in the Uzunakmat sheet based on bed length or area balancing meets problems due to a wide distribution of cleavage and similar folds, as well as the parallel trend of the map-scale fold axes and parallel extension axes of the strain ellipsoid, which imply changes in length and area of deformed beds in the cross-section plane. Therefore, the most reasonable method of shortening estimation is that discussed by Ramsay and Huber (1983), involving results of the strain analysis and calculation of the bed length correction coefficient ( $F$ -factor).

Estimation of shortening  $e = [(l_1 - l_0)/l_0] \times 100\%$  was done using initial  $l_0$  and modern  $l_1$  lengths between pin points within each domain. The axial ratio ( $R$ ) and angle ( $\varphi$ ) between the trace of bedding and extension axis in the cross-section plane were measured for each strain ellipsoid in the cross-section plane. Initial bed length ( $l_0$ ) was corrected in each domain by the  $F$ -factor:

$$F_l = (1 + \Delta_A)^{1/2} (R^{-1} + (R^2 - 1)R^{-1} \sin^2 \varphi)^{1/2}$$

where  $\Delta_A$  is area variation in the cross-section plane. This was calculated for each strain ellipsoid according to its shape and orientation (Ramsay and Huber, 1987).

Results of the shortening estimations within each domain are presented in Fig. 6. The total shortening calculated using only bed length balancing and that involving  $F$ -factor show similar trends, but balancing which involves  $F$ -factor shows much higher shortening values. The latter is the result of strain-related area decreasing due to extensional axes orientation parallel to map-scale fold axes and normal to cross-section plane. In total,  $F$ -factor involved balancing shows approximately 65% shortening near the CTT and 55% shortening near the TFF.

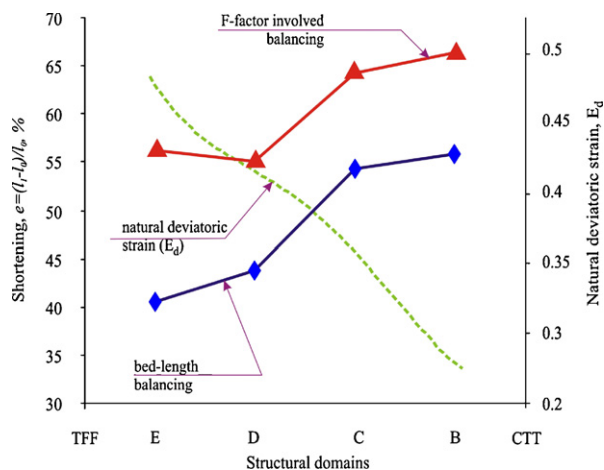


Fig. 6. Horizontal shortening values of the Uzunakmat sheet estimated by bed length balancing (blue line, no  $F$ -factor correction) and constant-volume balancing (red line,  $F$ -factor correction included).

Fig. 6. Valeurs du raccourcissement horizontal de l'unité d'Uzunakmat, estimé par ajustement de la longueur du banc (ligne bleue, pas de correction de facteur  $F$ ) et par ajustement à volume constant (ligne rouge, correction de facteur  $F$  incluse).

Gradual increase of shortening towards the CTT contrasts to decrease of natural deviatoric strain in the same direction (Fig. 6). It implies that beds in the frontal part of the Uzunakmat sheet close to the CTT were folded mainly by buckling without significant strain, whereas the internal part of the Uzunakmat sheet close to the TFF was affected by strain with regional-scale flattening but no intense folding. Differences in deformation mechanisms are likely explained by the structural thickening of internal parts of the Uzunakmat sheet and their burial to a greater depth likely resulted in an increase of the metamorphic grade toward the TFF (Frolova, 1982).

#### 5. Discussion and conclusion

Most of the observed features have already been documented in other fold and thrust belts or in physical modeling. For example, similar variations in strain magnitude and strain ellipsoid shape were discussed by Coward and Kim (1981), Paterson and Wainger (1991), Gray and Willman (1991). Distribution of local strain fields near map-scale faults is close to that in models by Osokina (2002) and Ma et al. (2007). However, the specific feature of the Uzunakmat sheet is that it is bounded by the TFF, i.e., a strike-slip-fault with significant displacement, which occurred long after the main deformation stages of the Talas Alatau area.

Relationship between the TFF and other structures of the Uzunakmat sheet, based on the data presented in this article, is summarized by the following main points:

- Elongation axes of strain ellipsoids, stretching lineation and map-scale fold axes are parallel to each other;
- Map-scale fold axial planes are parallel to thrusts and vary in dip from  $40^\circ$  to  $45^\circ$  near the CTT to subvertical near the TFF;

- Regional-scale faults including the CTT and TFF are parallel to each other;
- Natural deviatoric strain values gradually increases from the CTT to TFF;
- Shape of the strain ellipsoid gradually varies in each domain of the Usunakhmat sheet from oblate at the frontal thrust to prolate in internal parts of the unit.

Strong parallelism of small-scale- and map-scale structures including the CTT and TFF and their close connection with strain patterns show that they were formed during the same tectonic and metamorphic event, although occurrence of several sub-stages during the formation of a fold near the CTT has been proposed (Khudoley, 1993). Systematic dip variations of map-scale fold axial planes and thrust surfaces from the CTT to TFF also implies that they form a unique structural association. It implies that the TFF was formed during the main tectonic and metamorphic event as a part of a northeastward-vergent thrust and fold belt now represented by the Usunakhmat sheet and, probably, the Talas parautochthon.

The aforementioned data on the timing of deformation and the metamorphic event in the Usunakhmat sheet show that they likely occurred between Middle Ordovician and Early Devonian. Within the Malyi Karatau area, which is the northwestern structural continuation of the Talas Alatau region, thrusts and folds are cut by a Late Ordovician ( $448 \pm 4$  Ma) granite (Alexeiev et al., 2009). Combining data from the Talas Alatau and Malyi Karatau regions we infer that the main deformation and metamorphic event most likely occurred in Middle to Late Ordovician.

According to most common Early Paleozoic reconstructions, the Talas Alatau region was a part of the Kipchak island arc (Sengör and Natal'in, 1996). A study of phyllosilicates associated to the fold plane cleavages, shows a high pressure (at least 8 kbar)/low temperature (below 300 °C) metamorphism in the Uzunakhmat sheet, which is in accordance with a subduction related environment (Abad et al., 2003). Similarity in the structure of the Talas Alatau sedimentary basin with that of the Aleutian Trough was also discussed, although interpretation of the Talas Alatau region as an active margin meets some problems for local paleogeographic reconstructions (Khudoley and Semiletkin, 1992b). According to Burtman (2006), in the Early Paleozoic the Talas Alatau region was a part of the Syrdarya terrane which collided in Middle- to Late Ordovician with other terrains to build up the Kyrgyzian microcontinent.

The age of collision in the reconstruction by Burtman (2006) is in reasonable agreement with available data on the age of the Usunakhmat sheet deformation. The most likely formation of the TFF in the Talas Alatau region was related to the Ordovician collision event as well. During the Late Paleozoic the TFF was reactivated as a dextral strike-slip fault with displacement parallel to already formed folds and thrusts of the Usunakhmat sheet. Interpreting the TFF as an Early Paleozoic fault reactivated in Late Paleozoic explains why it does not show a cross-cutting relationship with the Early Paleozoic structures of the Usunakhmat sheet.

## Acknowledgements

Fruitful discussions with F. Yakovlev, N. Frolova, M. Goncharov, S. Semiletkin and other colleagues improved our knowledge of the regional geology and fold mechanics. K. Mulchrone and E. Erslev supplied the authors with software for strain analysis. D. Chew supplied with information on the precision of the  $R_f/\phi$  method. The authors are indebted to D. Alexeiev, A. Soloviev and the anonymous reviewer for constructive comments and suggestions. The research was partly supported by research grant from Saint Petersburg State University and Federal Program "Human Resources" project 14.740.11.0187.

## Appendix A. Supplementary data

Supplementary data (Table) associated with this article can be found, in the online version, at doi:10.1016/j.crte.2011.11.004.

## References

- Abad, I., Gutiérrez-Alonso, G., Nieto, F., Gertner, I., Becker, A., Cabero, A., 2003. The structure and the phyllosilicates (chemistry, crystallinity and texture) of Talas Ala-Tau (Tien Shan, Kyrgyz Republic): comparison with more recent subduction complexes. *Tectonophysics* 365, 103–127.
- Alexeiev, D.V., Cook, H.E., Buvtyshkin, V.M., Golub, L.Y., 2009. Structural evolution of the Ural–Tien Shan junction: a view from Karatau ridge, South Kazakhstan. *C. R. Geoscience* 341, 287–297.
- Bakirov, A., Dobretsov, N.L., 1972. Metamorphic Complexes of eastern Part of Middle Asia. Ilim, Frunze, 135 p. (in Russian).
- Becker, A.Y., 1987. On the relation between tectonic structures of the Uzunakhmat and Karaganian blocks of the Talas-Karatau structural-formation zone (Northern Tien Shan). In: Korolev, V.G. (Ed.), *Caledonides of Tien Shan*. Ilim, Frunze, (in Russian), pp. 21–36.
- Becker, A.Y., Makarov, V.A., Razboinikov, A.G., 1988. New data on the stratigraphy of Karagoin Group of the Talas Ala-Too (Northern Tien Shan). In: Kiselev, V.V. (Ed.), *Precambrian and Lower Paleozoic of Tien Shan*. Ilim, Frunze, (in Russian), pp. 100–126.
- Brandon, M.T., 1995. Analysis of geologic strain data in strain magnitude space. *J. Struct. Geol.* 10, 1375–1385.
- Burtman, V.S., 1975. Structural geology of the Variscan Tien Shan, USSR. *Am. J. Sci.* 272A, 157–186.
- Burtman, V.S., 1980. Faults of Middle Asia. *Am. J. Sci.* 280, 725–744.
- Burtman, V.S., 2006. Tien Shan and High Asia: Tectonics and Geodynamics of Paleozoic: *Transactions of Geological Institute*. Iss. 570. GEOS, Moscow, 216 p. (in Russian).
- Burtman, V.S., Skobelev, S.F., Molnar, P., 1996. Late Cenozoic slip on the Talas-Ferghana fault, the Tien Shan, Central Asia. *GSA Bull.* 108, 1004–1021.
- Chakabaev, S.E., 1979. Geological Map of Kazakh SSR Scale 1:500,000, South Kazakhstan series. *Aerogeologiya Map Enterprise*, Leningrad, USSR (in Russian).
- Chew, D.M., 2003. An Excel spreadsheet for finite strain analysis using the  $R_f/\phi$  technique. *Comput. Geosci.* 29, 795–799.
- M.P. Coward, J.H. Kim, Strain within thrust sheets. In: McClay K., Price N. (Eds.) *Thrust and Nappe Tectonics*. The Geological Society of London Special Publication 9, 1981, 275–292.
- Dunne, W.M., Onasch, C.M., Williams, R.T., 1990. The problem of strain marker centers of the Fry method. *J. Struct. Geol.* 7, 933–938.
- Erslev, E.A., Ge, H., 1990. Least-squares center-to-center and mean object ellipse fabric analysis. *J. Structural Geol.* 8, 1047–1059.
- Frolova, N.S., 1982. Influence of metamorphism on deformational properties of rocks (an example from Talas Ala Tau). *Geotectonics* 4, 18–24 (in Russian, translated in English).
- Goncharov, M.A., 1998. *The Mechanics of Geosyncline Folding*. Nauka, Moscow, 264 p. (in Russian).
- Gray, D.R., Willman, C.E., 1991. Thrust-related strain gradients and thrusting mechanisms in a chevron-folded sequence, southeastern Australia. *J. Struct. Geol.* 13, 691–710.

- Khudoley, A.K., 1993. Structural and strain analyses of the middle part of the Talassian Alatau ridge (Middle Asia, Kirgystan). *J. Struct. Geol.* 6, 693–706.
- Khudoley, A.K., Semiletkin, S.A., 1992a. Morphology and evolution of fold and fault structures of the Talass Alatau (Northern Tien-Shan). *Geotectonics* 1, 84–93 (in Russian, translated in English).
- Khudoley, A.K., Semiletkin, S.A., 1992b. Flysch basin of the Talass Alatau: paleocurrents and structure. *Lithol. Miner. Deposit.* 4, 51–62 (in Russian, translated in English).
- Kiselev, V.V., Korolev, V.G., 1981. Paleotectonics of the Tien Shan: Precambrian and Lower Paleozoic. *Ilim, Frunze*, 183 p. (in Russian).
- Kiselev, V.V., Apaiarov, F.H., Komarevzev, V.T., Ziganok, A.N., 1986. New data on U-Pb ages of stratificated rocks of the Tien Shan. In: *Method of Isotopic Geology and Geochronologic Scale*, Nauka, Moscow, pp. 215–225 (in Russian).
- Kiselev, V.V., Maksumova, R.A., 2001. Geology of the Northern and Middle Tien Shan: Principal outlines. In: Seltmann, R., Jenchuraeva, R. (Eds.), *Paleozoic Geodynamics and Gold Deposits in the Kyrgyz Tien Shan. International Geological Correlation Programme Excursion Guidebook*. Springer, Berlin, pp. 21–28.
- Ma, J., Liu, L.Q., Liu, P.X., Ma, S.L., 2007. Thermal precursory pattern on fault unstable slip: an experimental study of an echelon faults. *Chinese J. Geophys.* 4, 995–1004.
- Maksumova, R.A., Jenchuraev, A.V., Berezansky, A.V., 2001. Structure and evolution of thrust and fold complex of Kyrgyz Tien Shan. *Russian Geol. Geophys.* 10, 1444–1452 (in Russian, translated in English).
- Maluzhinetz, A.G., 1987. Metamorphic analogs of late flysch of Talas Alatau ridge and its depositional environment. In: *Sediment formation and its deposition environment*, IgiG SAS, Novosibirsk, pp. 134–149 (in Russian).
- Mulchrone, K.F., O'Sullivan, F., Meere, P.A., 2003. Finite strain estimation using the mean radial length of elliptical objects with bootstrap confidence intervals. *J. Structural Geol.* 4, 529–539.
- Onasch, C.M., 1984. Application of the  $Rf/\phi'$  technique to elliptical markers deformed by pressure solution. *Tectonophysics* 1–2, 157–165.
- Osokina, D.N., 2002. Stress field, fracturing and deformation mechanisms in fault zone. In: *Tectonophysics today*, IPE RAS, Moscow, pp. 129–174 (in Russian).
- Pastor-Galán, D., Gutiérrez-Alonso, G., Meere, P., Mulchrone, K., 2009. Factors affecting finite strain estimation in low-grade, low-strain clastic rocks. *J. Struct. Geol.* 31, 1586–1596.
- Paterson, S.R., Wainger, L., 1991. Strains and structures associated with a terrane bounding stretching fault: the Melones fault zone, central Sierra Nevada, California. *Tectonophysics* 1–2, 69–90.
- Ramsay, J.G., Huber, M.I., 1983. *The Techniques of Modern Structural Geology, V. 1: Strain Analysis*. Academic Press, London, 307 p.
- Ramsay, J.G., Huber, M.I., 1987. *The techniques of modern structural geology, V. 2: folds and fractures*. Academic Press, London, pp. 308–700.
- Sagyndykov, K.S., 1964. Metamorphism types and relation of Early Precambrian and Early Paleozoic complexes in Kok-lyrim-Too and Takhtalyk ridges. In: *Tectonics of Western part of northern Tien Shan*, Ilim, Frunze (in Russian).
- Semiletkin, S.A., 2007. Tectonics environment of Malyi Karatau and Talas Alatau flysch complexes based on Sm/Nd isotope and geochemistry studies. In: *Fundamental Problems of Geotectonics*, GEOS, Moscow, pp. 186–188 (in Russian).
- Sengör, A.M.C., Natal'in, B.A., 1996. Palaeotectonics of Asia: fragments and synthesis. In: Yin, A., Harrison, M. (Eds.), *The Tectonic Evolution of Asia*. Cambridge University Press, Cambridge, pp. 486–640.
- Tursungaziev, B.T., Petrov, O.P., 2008. *Geological Map of Kyrgyz Republic Scale 1:500,000*. VSEGEI, Saint Petersburg (in Russian).
- Voytenko, V.N., Khudoley, A.K., Gertner, I.F., 2006. Strain influence on chemical composition of sandstones (on examples of greenschist complex of the Talas Alatau, Kyrgyzstan). In: *Evolution of Tectonic Processes in Earth History*, GEOS, Moscow, pp. 140–142 (in Russian).
- Yakovlev, F.L., 1976. The role of the Central Talas thrust in geological structure of Karabura and Shilbillisai divide (northern Tien Shan). In: *Regional Geology of Some Areas of USSR*, Moscow University Publishing, Moscow, pp. 10–15 (in Russian).